DOI: 10.21776/ub.jpacr.2025.014.01.7933 *J. Pure App. Chem. Res.*, **2025**, 14 (1), 1-12
12 March 2025

# The Effect of Surfactant on the Characteristics of Curcumin-Loaded Nanostructured Lipid Carriers: Fluorescence and Stability Study

Mega Nurul Madania[1], Diah Mardiana[1], Ulfa Andayani[1], Anastasia Fitria Devi[2], and Zubaidah Ningsih[1*]

[1]Department of Chemistry, University of Brawijaya, Malang 65145, Indonesia
[2]Research Center for Chemistry, National Research and Innovation Agency (BRIN), Tangerang Selatan 15314, Indonesia

[*]Corresponding email: zubaidah@ub.ac.id

Received 06 December 2024; Accepted 03 January 2025

## ABSTRACT

Curcumin, a bioactive compound derived from *Curcuma longa*, offers significant pharmacological benefits such as antioxidant, anti-inflammatory, and anticancer properties. However, its therapeutic application is restricted due to poor water solubility, low systemic bioavailability, and limited skin penetration. This study explores the use of Nanostructured Lipid Carriers (NLCs) as a drug delivery system to improve curcumin's stability and permeability. Two formulations were developed: NLC-KUR-T80, which encapsulates curcumin using the non-ionic surfactant Tween 80, and NLC-KUR-CTAB, which uses the cationic surfactant CTAB. Both formulations were prepared using the Phase Inversion Temperature (PIT) method and characterized for particle size, polydispersity index (PI), zeta potential, encapsulation efficiency (EE%), and fluorescence properties. Results revealed that CUR-NLC-CTAB exhibited a larger particle size (1410 ± 183 nm), higher zeta potential (78.70 ± 0.67 mV), and significantly better encapsulation efficiency (27.33 ± 3.33%) compared to CUR-NLC-T80. Fluorescence studies demonstrated that curcumin within NLC-CTAB had enhanced fluorescence intensity, indicating better stability and distribution within the lipid matrix.

Keywords: Curcumin, Nanostructured Lipid Carrier (NLC), Tween 80, CTAB, Fluorescence

## INTRODUCTION

Curcumin is an active compound extracted from the rhizomes of Curcuma longa (turmeric), which belongs to the Zingiberaceae family. Curcumin is widely known for its pharmacological activities, such as anti-inflammatory [1], antioxidant [2], anticancer [3], antidiabetic [4], dan antibacterial [5]. Additionally, curcumin has potency in topical treatments, such as for skin disorders like psoriasis [6], acne [7] and in delaying the aging process [8]. However, its use in therapeutic applications is often limited by its poor water solubility [9], limited systemic bioavailability, and difficulty in skin penetration due to its hydrophobic nature [6], [10], [11].

One innovative approach to overcome these limitations is the development of the Nanostructured Lipid Carrier (NLC) drug delivery system, which enables the stabilization and distribution of curcumin within a lipid matrix. NLC contains a lipid matrix made from a mixture of solid and liquid lipids to form an amorphous, non-crystalline lipid core, which allows for higher drug loading [12], [13], [14]. In NLC formulations, the choice of surfactant is a critical

**The journal homepage www.jpacr.ub.ac.id**
**p-ISSN : 2302 – 4690 | e-ISSN : 2541 – 0733**

aspect that influences the characteristics of the NLC [15] and drug release [16]. Cationic surfactants, such as cetyltrimethylammonium bromide (CTAB), provide a high positive charge, which enhances the electrostatic stability of the particles [17], whereas non-ionic surfactants, such as Tween 80, tend to offer stability through steric mechanisms [18]. Elmowafy et al 16], and Putri et al [19]. have shown that the selection of surfactants can impact NLC characteristics, including particle size, stability, and encapsulation efficiency, nonetheless, their effects on the positioning or distribution of curcumin within the NLC system have not been intensively evaluated.

As a fluorophore, curcumin offers an advantage for a study using fluorescence techniques, since it enables us to detect changes in the polarity of its environment [20], [21]. In polar environments, curcumin fluorescence exhibits a shift in emission to longer wavelengths (red shift). In contrast, in nonpolar environments, the emission shifts to shorter wavelengths (blue shift) [22]. Fluorescence analysis provides high sensitivity to monitor the presence of curcumin and evaluate the interactions between the active molecule and the surrounding micro-environment.

Changes in the fluorescence properties of curcumin have been found to be useful for tracking its interactions with the environment [21] such as interactions with surfactants [23] and with cellular components. Fluorescence imaging of curcumin in cells provide quantitative data and also help to evaluate its intracellular localization [24], [25]. However, there has been limited research using fluorescence techniques to study the distribution of curcumin in an encapsulated system.

In this study, we explore the effects of cationic (CTAB) and non-ionic (Tween 80) surfactants on the characteristics of NLCs loaded with curcumin, including the distribution of curcumin in the system. By utilizing fluorescence techniques, this research offers a novel approach to understand the distribution of curcumin within the NLC system. Although this study focuses on the formulation and its effects on NLC characteristics, the results obtained may serve as an important foundation for future studies on biological applications.

## EXPERIMENT

### Chemicals and instrumentation

The chemicals used in this study include curcumin powder (Merck), stearic acid (Merck), soybean oil (Mamasuka), Tween 80 (Pharmaceutical Grade), cetyltrimethylammonium bromide (Merck), lecithin (Lansida), methanol (Smart Lab), aquadest, and ice blocks purchased from a local market.

The instrumentations used in this study include a set of phase inversion temperature equipment (Hot plate Magnetic Stirrer (Heidolph), oil bath, water bath, alcohol thermometer (SK SATO)), stereo microscope with digital camera (Olympus BX51), Zetasizer Pro Red Label (Malvern Panalytical), Ultrasonic Cleaner 40 kHz (Skymen), UV-Vis Spectrophotometer 1601, 220 V (Shimadzu), Fluorescence Microscope (Olympus IX-71), Nanodrop 3300 spectrofluorometer (Thermo Fisher), and a set of chemical glassware, ImageJ Software version 1.44.

### Procedure reaction

### Preparation and characterization of CUR-NLC

### Preparation of CUR-NLC

NLC was prepared using the phase inversion temperature (PIT) method, following the previous study by Calligaris et al. [26] with some modifications. Initially, the oil phase was



The journal homepage www.jpacr.ub.ac.id
p-ISSN : 2302 – 4690 | e-ISSN : 2541 – 0733

prepared by dispersing curcumin into a mixture of solid lipid (stearic acid), liquid lipid (soybean oil), and lecithin at a temperature of 75-80°C. In a separate vial, the aqueous phase was prepared by dissolving the surfactant (Tween 80 or CTAB) in distilled water. After both phases were heated, the aqueous phase was added to the oil phase to form a homogeneous emulsion. The emulsion was then processed using the phase inversion temperature (PIT) method for a single cycle, consisting of one heating and one cooling step. The heating process involved stirring the sample in an oil bath for 30 minutes at 85-90°C, followed by rapid cooling in an ice bath for 5 minutes. The concentration of ingredients in the sample formula was determined based on sample stability and high encapsulation efficiency from the preliminary tests. The formulation composition is presented in Table 1.

**Table 1.** Compositions of of curcumin loaded NLC formulations

| Material | % w/w |
|---|---|
| Curcumin | 0.428 |
| Stearic acid | 0.411 |
| Soybean oil | 2.691 |
| Lechitin | 1.542 |
| Surfactant (Tween 80 or CTAB) | 9.237 |
| Aquadest | 85.690 |

**Particle size, polydispersity index, and zeta potential measurement**

The average particle size (Z-average) and polydispersity index (PI) of CUR-NLC were measured using the Zetasizer Pro Red Label (Malvern Panalytical) with the Dynamic Light Scattering (DLS) technique. Water was used as the dispersant, with a refractive index of 1.33, viscosity of 0.887 cP, and dielectric constant of 78.5 [19]. The zeta potential (ZP) of the particles was measured using the same instrument, equipped with Phase Analysis Light Scattering (PALS) in Mixed Mode Measurement (M3) mode. Prior to measurement, the sample was diluted in water with a 25x dilution factor. Measurements of particle size and zeta potential were conducted at 25°C, with three repetitions to obtain the mean values of Z-average, PI, and ZP.

**Encapsulation Efficiency of CUR-NLC**

Briefly, CUR-NLC was diluted and then centrifuged at 3500 rpm for 45 minutes to separate the non-encapsulated curcumin from the NLC particles. A total of 5 ml of the supernatant was collected as the free curcumin fraction. The remaining filtrate, representing total curcumin, was diluted with methanol at a 1:1 ratio and then sonicated for 5 minutes to break down the NLC particles. The concentrations of free curcumin and total curcumin were measured using a UV-Vis spectrophotometer at a wavelength of 420 nm. The Encapsulation Efficiency (EE%) of curcumin encapsulated in the NLC was then calculated using the appropriate Eqs (1) [19]:

$$\%EE = \frac{[total\ curcumin]-[free\ curcumin]}{[total\ curcumin]} \text{ x } 100\% \qquad (1)$$

**Storage stability of CUR-NLC**

The stability of the CUR-NLC samples was evaluated at a storage temperature of 8°C (±1°C) over a 14-day period [19]. The purpose of this test was to assess the sample's physical



The journal homepage www.jpacr.ub.ac.id
p-ISSN : 2302 – 4690 | e-ISSN : 2541 – 0733

ability under storage conditions. The observed physical stability parameters including morphology and visual inspection. The morphology of CUR-NLC was examined using a stereo microscope with a digital camera (Olympus BX51, Japan) at 400x magnification. Several images were captured to observe the morphology and particle size distribution.

**Observation of curcumin distribution in NLC**

The morphology and intensity of curcumin in NLC were observed using fluorescence microscopy. CUR-NLC samples were prepared on glass slides. The morphology and intensity of CUR-NLC were examined under a 40x objective lens magnification, utilizing a green filter lamp and auto-exposure mode. Several images were captured to analyze the morphological distribution of CUR-NLC.

**Measurement of fluorescence intensity of curcumin in NLC**

The fluorescence emission spectrum of curcumin in NLC was measured using a Nanodrop 3300 spectrofluorometer. Measurements were conducted at an emission wavelength of 539 nm, with a blue filter lamp as the excitation source, operating at a maximum excitation wavelength range of 470 nm. The Nanodrop spectrofluorometer was interfaced with computer software for data acquisition. The measurement process began with aquadest as a blank solution, followed by the NLC sample. A volume of 1–2 µL of the solution was placed on the bottom pedestal column of the Nanodrop instrument, which was then covered with the top column. Using the computer software, the "blank" button was clicked for the blank solution, and the "measure" button was used for the sample. After each measurement, the bottom pedestal column was cleaned thoroughly to prevent cross-contamination. The results were displayed as a graph of emission spectrum illustrating the relationship between emission intensity or relative fluorescence units (RFU) and wavelength (nm).

## RESULT AND DISCUSSION

### Characterization of CUR-NLC

**Particle size, polydispersity index, zeta potential, and encapsulation efficiency of CUR-NLC**

This study focuses on the effect of cationic (CTAB) and non-ionic (T80) surfactants on the characteristics of NLC, as well as determining the impact of the surface charge of NLC on drug delivery through the modeled skin. Table 2 presents the characteristics of two NLC formulations containing curcumin. Particle size and distribution, as well as zeta potential, are important characteristics that can influence the stability, solubility, release rate, and biological performance of NLC. The NLC typically have a diameter ranging from 10 to 1000 nm [27].

The average particle size of CUR-NLC-T80 is 165.5 ± 48.9 nm with a polydispersity index (PI) of 0.487 ± 0.135. In contrast, CUR-NLC-CTAB yields an average particle size of 1410 ± 183 nm with a PI of 1. The PI for both NLC formulations is greater than 0.3, indicating a less homogeneous particle size distribution [27]. CUR-NLC-CTAB exhibits a highly heterogeneous particle size distribution ranging from nano to micro sizes, compared to the CUR-NLC-T80 particle sizes, which remain predominantly within the nanometer size. As a representative example, Figure 1 shows the morphology of particles for both NLC formulations on day 0.

In addition, ZP can reflect surface charge, affinity for surrounding ions, and particle stability. Particles with a ZP of ±30 mV are considered to have good stability [28], [29], [30]. The ZP can be influenced by the type of surfactant and the particle environment, including the



The journal homepage www.jpacr.ub.ac.id
p-ISSN : 2302 – 4690 | e-ISSN : 2541 – 0733

types of ions present, ionic strength, and pH [27]. The two NLC formulations, CUR-NLC-T80 and CUR-NLC-CTAB, exhibit different zeta potential values. The negative charge (-27.80 ± 0.08 mV) in the CUR-NLC-T80 formulation can be attributed to the presence of certain anionic contaminants (e.g., free fatty acids) in Tween 80 as a commercial surfactant product [31]. Our measurement shows that the mixture of commercial T80 and lecithin applied in this research gives non zero conductivity (19.86 µS/cm) signifying the presence of contaminant which shows surface-activity. Meanwhile, the CUR-NLC-CTAB formulation has a relatively high positive charge (78.70 ± 0.67 mV), which is due to the presence of the positively charged head of CTAB, resulting in a positively charged surface of the NLC particles [32].

The encapsulation efficiency percentage (EE%) is defined as the percentage of the drug that is successfully encapsulated within lipid nanoparticles or micelles [33]. The %EE is 27.333 ± 3.334% for CUR-NLC-CTAB, while it is 4.110 ± 1.810% for CUR-NLC-T80. The higher EE% observed in CUR-NLC-CTAB indicates that CTAB can facilitate a greater encapsulation of curcumin within the NLC compared to T80. This finding is consistent with previous research reported by Putro et al., which noted that the drug loading content using cationic surfactants is higher than that using non-ionic surfactants [34].

**Table 2.** Average particle size (Z-average), polydispersity index (PI), zeta potential (ZP), and encapsulation efficiency percentage (EE%) (mean ± SD, n = 3) of the NLC formulation containing curcumin.

| Code sample | Z-average (nm) | PI | ZP (mV) | EE% |
|---|---|---|---|---|
| CUR-NLC-T80 | 165.6 ± 48.9 | 0.487 ± 0.135 | -27.80 ± 0.08 | 4.110 ± 1.810 |
| CUR-NLC-CTAB | 1410 ± 183 | 1.000 ± 0.000 | 78.70 ± 0.67 | 27.333 ± 3.334 |

**Morphology and Storage stability**

The stability of CUR-NLC formulations prepared with two surfactants of differing ionic profiles was evaluated. Microscopic morphological observations in Figure 1 show that NLC particles are in spherical shape. Stability assessments were conducted daily over 4 days (Figure 1) and weekly over a 14-days period (Figure 2). Visual inspection on day 0 showed that CUR-NLC-T80 was clearer and more transparent, while CUR-NLC-CTAB appeared to be more turbid and viscous, as seen in Figure 2. This difference is attributed to the larger and more heterogeneous particle size of CUR-NLC-CTAB compared to CUR-NLC-T80, which is in agreement with measurements of sample's particle size.

Daily stability observations of CUR-NLC samples are illustrated in Figure 1. CUR-NLC-T80 begins to lose stability on day 1, with the solution turning cloudy yellow, followed by sedimentation on day 2. Meanwhile, CUR-NLC-CTAB exhibited instability by day 4, as evidenced by phase separation. This instability can be further clarified through microscopic observations, which show a progressive increase in particle size for both CUR-NLC-T80 and CUR-NLC-CTAB. The instability of CUR-NLC-CTAB was also indicated by the release of curcumin from the lipid matrix. The instability of CUR-NLC-CTAB is also indicated by the presence of a dark orange crystal structure pattern which likely indicates the release of curcumin from the lipid matrix. Prolonged storage up to 7 and 14 days further contributed to the increasing instability of both CUR-NLC samples, as shown in Figure 2. Factors that may affect instability are PI and zeta potential. PI values of CUR-NLC-T80 and CUR-NLC-CTAB greater than 0.3 indicate non-uniformity of particle size distribution. This size non-uniformity



The journal homepage www.jpacr.ub.ac.id
p-ISSN : 2302 – 4690 | e-ISSN : 2541 – 0733

can accelerate the Oswald ripening phenomenon, which is when small particles combine with larger particles, causing the particles to grow larger [31], [35], [36]. Furthermore, CUR-NLC-CTAB showed a very high zeta potential (78.70 ± 0.67) compared to CUR-NLC-T80 (-27.80 ± 0.08). Although the zeta potential of CUR-NLC-CTAB increased to very positive, the dispersion stability did not last long. This is due to the electrical double layer (EDL) compression phenomenon. When the EDL is compressed due to excessive surfactant concentration, the electrostatic repulsion force becomes weaker, thereby reducing the stability of the colloid. As a result, although the zeta potential becomes higher, the repulsive interactions between particles are not strong enough to prevent aggregation or precipitation [35].

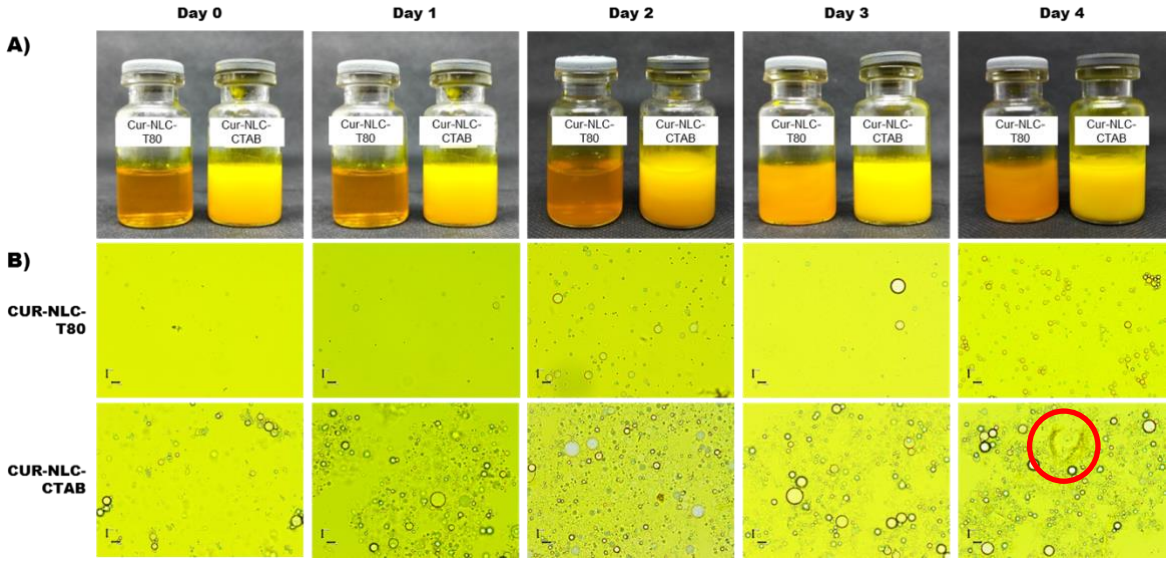


**Figure 1.** Representation of CUR-NLC samples per day during 4 days of storage: (A) Visual image of CUR-NLC, (B) image of the microscopic morphology of CUR-NLC at 400x magnification using a digital imaging microscope (scale bar = 10 µm)

**Observation of curcumin distribution in NLC**

The NLC system employs a solubilization technique, encapsulating hydrophobic curcumin within the hydrophobic core of the NLC. The hydrophobic tails of surfactant molecules surround and protect the curcumin from the aqueous medium. Consequently, the interaction between curcumin and the surfactant may involve both electrostatic and hydrophobic forces, which play a critical role in determining the localization of curcumin within the NLC system [37].

The morphological observation of CUR-NLC using fluorescence microscopy was conducted to examine the physical characteristics of curcumin encapsulated within the NLC. Fluorescence microscopy utilizes the intrinsic fluorescence properties of curcumin, which emits light at specific wavelengths, allowing curcumin to appear as green fluorescent particles [38]. The green fluorescence intensity of curcumin can indicate its presence within the NLC system, as seen in Figure 3.



The journal homepage www.jpacr.ub.ac.id
p-ISSN : 2302 – 4690 | e-ISSN : 2541 – 0733

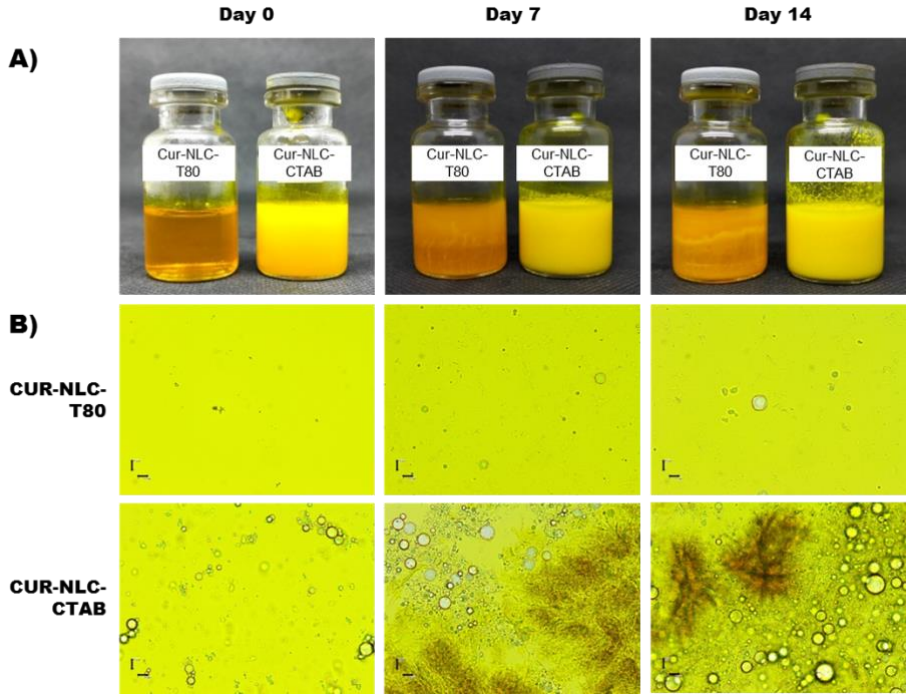


**Figure 2.** Representative CUR-NLC samples per week for 14 days of storage: (A) Visual image of CUR-NLC, (B) image of the microscopic morphology of CUR-NLC at 400x magnification using a digital imaging microscope (scale bar = 10 μm)


**Figure 3.** Imaging of curcumin. (A) NATIVECUR, (B) CUR-NLC-T80, (C) CUR-NLC-CTAB

Morphologically, CUR-NLC-CTAB particles are spherical with uneven particle sizes. The fluorescence intensity of curcumin is generally higher at the surface of the NLC, indicating that curcumin is primarily concentrated at the outer layer of the NLC. In smaller NLC particles, curcumin is distributed more evenly throughout the particle, while in larger NLC particles, the interior is relatively darker indicating a lower fluorescence intensity of curcumin. This difference can be attributed to the particle size, which affects the ability of curcumin to be distributed uniformly [39]. Additionally, the presence of fluorescence intensity outside the NLC suggests that some curcumin may not have been successfully encapsulated. These findings indicate that optimization of the formulation and encapsulation process is necessary to achieve a more uniform distribution of curcumin with high encapsulation efficiency within the NLC structure.



The journal homepage www.jpacr.ub.ac.id
p-ISSN : 2302 – 4690 | e-ISSN : 2541 – 0733

In the morphological observation of CUR-NLC-T80, identifying the distribution of curcumin in the system is challlenging due to the minuscule size of the NLC particles prohibiting a clear image of curcumin position and distribution. Thus, we combine the observation of curcumin fluorescence image together with the emission spectrum measured using spectrofluorometer to obtain clearer description of curcumin distribution in the system.

**Fluorescence intensity of curcumin in NLC**

Curcumin is known as a molecule with fluorescence properties sensitive to the polarity of its environment. Changes in the polarity of the environment can affect both the emission peak position and the fluorescence intensity. In a non-polar environment, curcumin tends to have higher emission intensity, in contrast, curcumin has lower emission intensity in polar environment due to energy release through non-radiative relaxation [21].

Figure 4 illustrates the emission spectra of curcumin dissolved in water (NATIVE-CUR) and curcumin encapsulated within NLC. The changes in the spectral shape and the shift in the maximum emission peak indicate an alteration in the curcumin environment. CUR-NLC causes a shift in the fluorescence emission peak to a shorter wavelength compared to NATIVE-CUR. NATIVE-CUR exhibits a broad fluorescence peak at 574 nm [40], [41]. For CUR-NLC, the fluorescence peak shift is observed at wavelengths of 504 and 534 nm for the CUR-NLC-CTAB system, and at 509 and 534 nm for the CUR-NLC-T80 system. The emission peak at 574 nm remains detectable in CUR-NLC, but its intensity is less dominant. This shift, known as a blue shift, indicates a change in the curcumin environment from a highly polar aqueous medium to a more non-polar environment within the NLC matrix [40]. As a lipophilic compound, curcumin has high solubility in oils (non-polar) but low solubility in water [42]. In the NLC system, curcumin can interact with the oil phase as well as the hydrophilic surfactant alkyl chains [43].

In addition to the shift in the emission peak, differences in fluorescence intensity were also observed between curcumin in the NATIVE-CUR and CUR-NLC forms. NATIVE-CUR exhibits high fluorescence intensity at wavelengths of 574 nm (97 RFU) and 499 nm (191 RFU). In the CUR-NLC-CTAB system, fluorescence intensity increases compared to NATIVE-CUR. In contrast, in the CUR-NLC-T80 system, a significant decrease in fluorescence intensity of curcumin is observed. These changes in fluorescence intensity, whether an increase or a decrease, can be influenced by interactions of curcumin with surfactants (CTAB and T80), the Excited State Intramolecular Proton Transfer (ESIPT) process, quenching mechanisms, and solution viscosity [41], [44], [45].

The aryl group in curcumin exhibits strong interactions with the saturated alkyl chains of CTAB, creating a hydrophobic environment and enhancing the emission intensity of curcumin. This strong hydrophobic interaction can inhibit the Excited State Intramolecular Proton Transfer (ESIPT) process, a proton transfer mechanism that occurs between the hydroxyl and keto groups of the cis-enol tautomer in curcumin molecules when in the excited state. This process influences how energy is released from the excited state, including the fluorescence intensity produced. Inhibition of ESIPT in the CTAB system leads to an increase in curcumin's fluorescence intensity. In contrast, the presence of unsaturation (double bonds) in the alkyl chain of Tween 80 tends to reduce its hydrophobic interaction with the aryl groups of curcumin. This condition enhances hydration at the Tween 80 surfactant interface, which then facilitates the ESIPT process of curcumin. When ESIPT occurs more efficiently, the energy absorbed by curcumin is released through proton transfer mechanisms as non-radiative energy. As a result, the fluorescence intensity of curcumin decreases because the absorbed energy is not emitted as



The journal homepage www.jpacr.ub.ac.id
p-ISSN : 2302 – 4690 | e-ISSN : 2541 – 0733

light but rather dissipated through the ESIPT process. This decrease in fluorescence intensity is directly related to the reduced of curcumin emission intensity [41].

The decrease in fluorescence intensity observed in CUR-NLC-T80 may be attributed to the formation of hydrogen bonds between curcumin and Tween 80. The hydroxyl group in Tween 80 allows for hydrogen bonding with polar groups on curcumin, such as the phenolic and enolic groups [44]. This interaction results in the formation of a nonfluorescent complex, leading to a static quenching mechanism. In static quenching, some fluorophores become undetectable because the complex molecules formed in the ground state absorb photons, and after excitation, return to the ground state without emitting fluorescence. Additionally, oxygen acts as a quencher by removing energy from curcumin through non-radiative energy transfer, subsequently forming a nonfluorescent complex. This phenomenon reduces the fluorescence intensity of curcumin in the CUR-NLC-T80 system [45].

An increase in solution viscosity can enhance the fluorescence intensity of curcumin. CUR-NLC-CTAB exhibits higher viscosity compared to CUR-NLC-T80, which results in a higher fluorescence intensity. When curcumin is in the ground state, bond rotation in the molecule is hindered by a significant energy barrier. However, in the excited state, this energy barrier is reduced, allowing bond rotation in curcumin to occur more rapidly. Rapid rotation in the excited state enables curcumin molecules to return to the ground state more quickly, with less energy loss through non-radiative processes. As a result, more energy can be released in the form of light, contributing to the increase in fluorescence intensity [45].

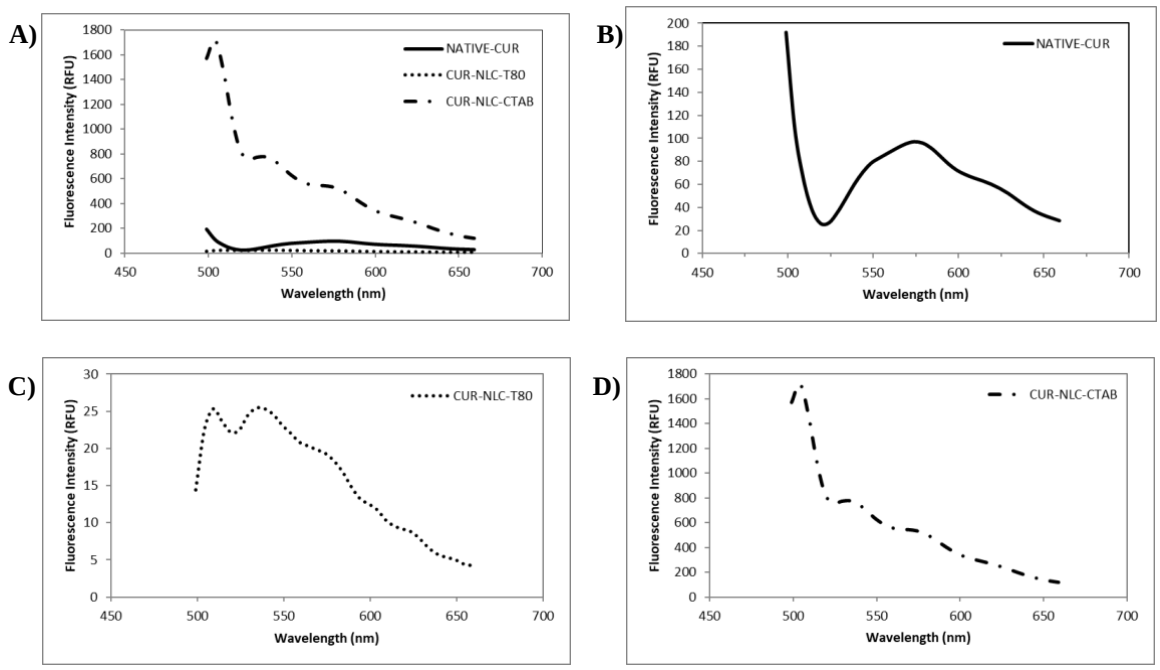


**Figure 4.** (A) combination of several emission spectra of curcumin in various formulations, (B) emission spectra of NATIVE-CUR (C) emission spectra of CUR-NLC-T80, (D) emission spectra of CUR-NLC-CTAB



The journal homepage www.jpacr.ub.ac.id
p-ISSN : 2302 – 4690 | e-ISSN : 2541 – 0733

## CONCLUSION

The results indicate that the type of surfactant influences particle size, zeta potential, encapsulation efficiency, and the distribution of curcumin within the NLC system. The choice of surfactant (CTAB or Tween 80) affects the microenvironment of curcumin, as reflected in the intensity and position of the emission spectra. CTAB produces particles with higher encapsulation efficiency and fluorescence intensity compared to Tween 80, which reflects the differences in the interactions between curcumin molecules and the components in the NLC. Curcumin is more uniformly distributed within the NLC with smaller particle sizes, whereas in larger particles, fluorescence intensity is more dominant at the surface, indicating a higher concentration of curcumin in that region.

## ACKNOWLEDGMENT

The authors are thankful to Universitas Brawijaya for providing an internal grant (Doctoral Grant) 2024 for this research work. The authors also acknowledge the National Research and Innovation Agency (BRIN) for supporting this research through Barista Program providing thesis project research funding.

## REFERENCES

[1] Peng, Y., Ao, M., Dong, B., Jiang, Y., Yu, L., Chen, Z., Hu, C., Xu, R. *Drug Des. Devel. Ther.*, **2021**, *15*, 4503–4525.
[2] Jakubczyk, K., Drużga, A., Katarzyna, J., Skonieczna-Żydecka, K. *Antioxidants*, **2020**, *9* (11), 1092.
[3] Baldi, A., De Luca, A., Maiorano, P., D'Angelo, C., Giordano, A. *Int. J. Mol. Sci.*, **2020**, *21* (5), 1839.
[4] Quispe, C., Herrera-Bravo, J., Javed, Z., Khan, K., Raza, S., Gulsunoglu-Konuskan, Z., Daştan, S. D., Sytar, O., Martorell, M., Sharifi-Rad, J., Calina, D. *BioMed Res. Int.*, **2022**, *2022* (1), 1375892.
[5] Teow, S.-Y., Liew, K., Ali, S. A., Khoo, A. S.-B., Peh, S.-C. *J. Trop. Med.*, **2016**, *2016*, e2853045.
[6] Boscariol, R., Caetano, É. A., Grotto, D., Rosa-Castro, R. M., Oliveira Junior, J. M., Vila, M. M. D. C., Balcão, V. M. *Pharmaceutics*, **2022**, *14* (4), 779.
[7] Rapalli, V. K., Kaul, V., Waghule, T., Gorantla, S., Sharma, S., Roy, A., Dubey, S. K., Singhvi, G. *Eur. J. Pharm. Sci.*, **2020**, *152*, 105438.
[8] Bahrami, A., Montecucco, F., Carbone, F., Sahebkar, A. *BioMed Res. Int.*, **2021**, *2021* (1), 8972074.
[9] Jannah, M., Lestari, M. L. A. D., Yanti, E. I., Ningsih, Z. *AIP Conf. Proc.*, **2021**, *2360* (1), 050005.
[10] Suresh, K., Nangia, A. *CrystEngComm*, **2018**, *20* (24), 3277–3296.
[11] Kriplani, P., Guarve, K., Singh Baghel, U. *Chin. Herb. Med.*, **2021**, *13* (2), 274–285.
[12] Ferreira, K. C. B., Valle, A. B. C. dos S., Paes, C. Q., Tavares, G. D., Pittella, F. *Pharmaceutics*, **2021**, *13* (9), 1454.
[13] Won, J.-H., Jin, M., Na, Y.-G., Song, B., Yun, T.-S., Hwang, Y.-R., Lee, S.-R., Je, S., Kim, J.-Y., Lee, H.-K., Cho, C.-W. *J. Drug Deliv. Sci. Technol.*, **2023**, *89*, 105108.
[14] Zhang, J., Chuesiang, P., Kim, J. T., Shin, G. H. *Food Chem.*, **2022**, *392*, 133306.
[15] Han, F., Li, S., Yin, R., Liu, H., Xu, L. *Colloids Surf. Physicochem. Eng. Asp.*, **2008**, *315* (1), 210–216.



The journal homepage www.jpacr.ub.ac.id
p-ISSN : 2302 – 4690 | e-ISSN : 2541 – 0733

[16] Elmowafy, M., Shalaby, K., Ali, H. M., Alruwaili, N. K., Salama, A., Ibrahim, M. F., Akl, M. A., Ahmed, T. A. *Int. J. Pharm.*, **2019**, *572*, 118781.
[17] Tran, T., Gonzalez Perdomo, M. E., Haghighi, M., Amrouch, K. *Geoenergy Sci. Eng.*, **2023**, *228*, 212041.
[18] Zhao, S., Yang, X., Garamus, V. M., Handge, U. A., Bérengère, L., Zhao, L., Salamon, G., Willumeit, R., Zou, A., Fan, S. *Langmuir*, **2014**, *30* (23), 6920–6928.
[19] Putri, E. F. A., Indahyanti, E., Mardiana, D., Lestari, M. L. A. D., Ningsih, Z. *Sci. Technol. Indones.*, **2023**, *8* (3), 509–515.
[20] de França, B. M., Oliveira, S. S. C., Souza, L. O. P., Mello, T. P., Santos, A. L. S., Bello Forero, J. S. *Dyes Pigments*, **2022**, *198*, 110011.
[21] Priyadarsini, K. I. *J. Photochem. Photobiol. C Photochem. Rev.*, **2009**, *10* (2), 81–95.
[22] Patra, D., Barakat, C. *Spectrochim. Acta. A. Mol. Biomol. Spectrosc.*, **2011**, *79* (5), 1034–1041.
[23] Mondal, S., Ghosh, S. *J. Photochem. Photobiol. B,* **2012**, *115*, 9–15.
[24] Kunwar, A., Barik, A., Pandey, R., Priyadarsini, K. I. *Biochim. Biophys. Acta BBA - Gen. Subj.*, **2006**, *1760* (10), 1513–1520.
[25] Kunwar, A., Barik, A., Mishra, B., Rathinasamy, K., Pandey, R., Priyadarsini, K. I. *Biochim. Biophys. Acta BBA - Gen. Subj.*, **2008**, *1780* (4), 673–679.
[26] Calligaris, S., Valoppi, F., Barba, L., Pizzale, L., Anese, M., Conte, L., Nicoli, M. C. *Food Biophys.*, **2017**, *12* (1), 45–51.
[27] Khosa, A., Reddi, S., Saha, R. N. *Biomed. Pharmacother.*, **2018**, *103*, 598–613.
[28] Fatfat, Z., Karam, M., Maatouk, B., Fahs, D., Gali-Muhtasib, H. In *Advanced and Modern Approaches for Drug Delivery*, Nayak, A. K., Hasnain, M. S., Laha, B., Maiti, S., Eds., Academic Press,, **2023**, 159–197.
[29] Samimi, S., Maghsoudnia, N., Eftekhari, R. B., Darkoosh, F. Lipid-Based Nanoparticles for Drug Delivery Systems, *in* book Mohapatra, S. S., Ranjan, S., Dasgupta, N., Mishra, R. K., Thomas, S., Characterization and Biology of Nanomaterials for Drug Delivery, **2019**, Elsevier.
[30] Smith, M. C., Crist, R. M., Clogston, J. D., McNeil, S. E. *Anal. Bioanal. Chem.*, **2017**, *409* (24), 5779–5787.
[31] Kharat, M., Zhang, G., McClements, D. J. *Food Res. Int.*, **2018**, *111*, 178–186.
[32] Rostinawati, T., Sriwododo, Susilawati, Y., Yohana Ch, A. *J. Kartika Kim.*, **2022**, *5* (1), 79–89.
[33] Ong, S. G. M., Ming, L. C., Lee, K. S., Yuen, K. H. *Pharmaceutics*, **2016**, *8* (3), 25.
[34] Putro, J. N., Ismadji, S., Gunarto, C., Soetaredjo, F. E., Ju, Y. H. *J. Mol. Liq.*, **2020**, *298*, 112034.
[35] Rosen, M. J. Surfactants and Interfacial Phenomena, **1978**, John Wiley & Sons, United States.
[36] Wu, L., Zhang, J., Watanabe, W. *Adv. Drug Deliv. Rev.*, **2011**, *63* (6), 456–469.
[37] Maity, B., Chatterjee, A., Ahmed, S. A., Seth, D. *J. Phys. Chem. B*, **2015**, *119* (9), 3776–3785.
[38] Akbari, E., Akhavan, O., Hatamie, S., Rahighi, R. *J. Drug Deliv. Sci. Technol.*, **2018**, *45*, 422–427.
[39] Hakim, L., Mardiana, D., Rokhiyah, U., Lestari, M. L. A. D., Ningsih, Z. *Sci. Technol. Indones.*, **2021**, *6* (3), 113–120.
[40] Patra, D., Barakat, C. *Spectrochim. Acta. A. Mol. Biomol. Spectrosc.*, **2011**, *79* (5), 1034–1041.



The journal homepage www.jpacr.ub.ac.id
p-ISSN : 2302 – 4690 | e-ISSN : 2541 – 0733

[41] Wang, X., Gao, Y. *Food Chem.*, **2018**, *246*, 242–248.
[42] Urošević, M., Nikolić, L., Gajić, I., Nikolić, V., Dinić, A., Miljković, V. *Antibiotics*, **2022**, *11* (2), 135.
[43] Santiago, R. R., Gyselle de Holanda e Silva, K., Dantas dos Santos, N., Genre, J., Freitas de Oliveira Lione, V., Silva, A. L., Marcelino, H. R., Gondim, A. D., Tabosa do Egito, E. S. *J. Drug Deliv. Sci. Technol.*, **2018**, *48*, 372–382.
[44] Rana, A. A., Yusaf, A., Shahid, S., Usman, M., Ahmad, M., Aslam, S., Al-Hussain, S. A., Zaki, M. E. A. *Pharm. Basel Switz.*, **2023**, *16* (12), 1663.
[45] Lakowicz, J. R. Principles of Fluorescence Spectroscopy, **2006**, Springer, New York.



The journal homepage www.jpacr.ub.ac.id
p-ISSN : 2302 – 4690 | e-ISSN : 2541 – 0733